Computational study on the iodobenzene-catalyzed oxidative cyclization of a δ-alkynyl β-ketoester

Smaher E. Butt,[a] Arantxa Rodríguez,[a] Jean-Marc Sotiropoulos,[b]* and Wesley J. Moran[a]*

[a] Department of Chemical Sciences, University of Huddersfield, Queensgate, Huddersfield HD1 3DH, U. K.
[b] Université de Pau et des Pays de l'Adour, IPREM (CNRS-UMR 5254), Technopole Hélioparc, 2 Avenue du Président Pierre Angot, 64053 Pau Cedex 09, France
Email: jean-marc.sotiro@univ-pau.fr; w.j.moran@hud.ac.uk

Abstract

The iodobenzene-catalyzed oxidative cyclization of a δ-alkynyl β-ketoester has been investigated by density functional theory (DFT) calculations at the $CPCM_{(acetonitrile)}/B3LYP/6-311++G(d,p)//B3LYP/SDD(I)$ levels. Three different mechanisms were considered for this process, and of the three, activation of the alkyne by a hypervalent iodine species followed by cyclization was found to be the most likely pathway based upon our computational results.
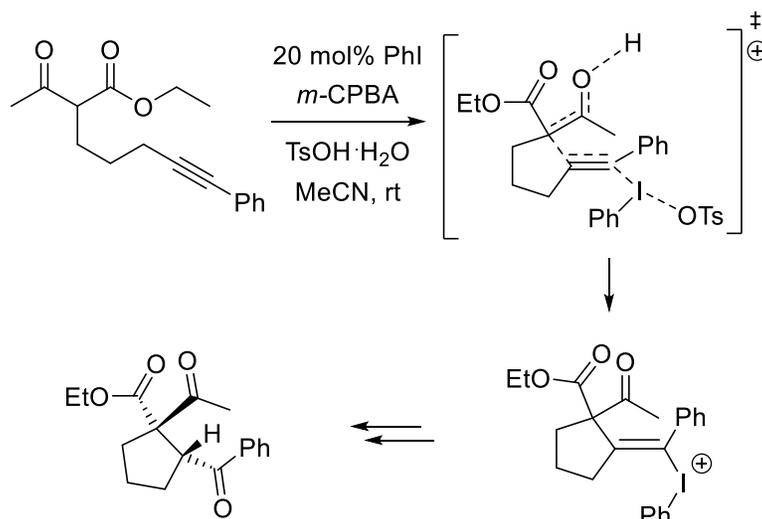
**Keywords:** Hypervalent iodine, DFT, alkyne, cyclization

Introduction

Hypervalent iodine chemistry has enjoyed significant attention in recent years and many studies have been reported over the last decades.[1-4] In particular, a plethora of new reactions and modes of reactivity have been uncovered, including examples of catalysis and enantioselective transformations. Hypervalent iodine species can effect transformations that would otherwise require transition metal catalysts or heavy metal oxidants but without the cost, supply or toxicity issues. Our collective understanding of these hypervalent iodine mediated processes has also increased, however there are still many mechanistic peculiarities that are poorly understood. In this regard, several computational studies have been described that have finally shone light on some of the intriguing mechanisms mediated by hypervalent iodine species.[5-8] In 2015, we reported that hypervalent iodine species can induce cyclization of *N*-allylbenzamides to give 2-oxazolines.[9] Subsequently, we reported our computational and kinetic experiments that suggested that this process proceeded through alkene activation (Scheme 1a).[10] Intriguingly, our studies on the cyclization of *N*-allylbenzamide **1** suggested that a molecule of trifluoroacetic acid is necessary, alongside the iodine(III) species, for efficient cyclization to occur. We also demonstrated that 2-iodoanisole is a superior catalyst to iodobenzene with a 1.7 kcal.mol^{-1} difference in activation energy, which supported our experimental observations. We did not consider this mechanism to be particularly contentious, although we did rule out an alternative mechanism involving amide activation by the iodine(III) followed by attack of the alkene. In 2011, we reported the cyclization of δ-alkynyl β-ketoesters, e.g. **3**, to cyclopentanes, e.g. **4**, for which more than one reasonable mechanism can be proposed (Scheme 1b).[11] In this case, a C-C bond is formed which is relatively uncommon by hypervalent iodine reagents.[12]

(a) Previous work: alkene activation
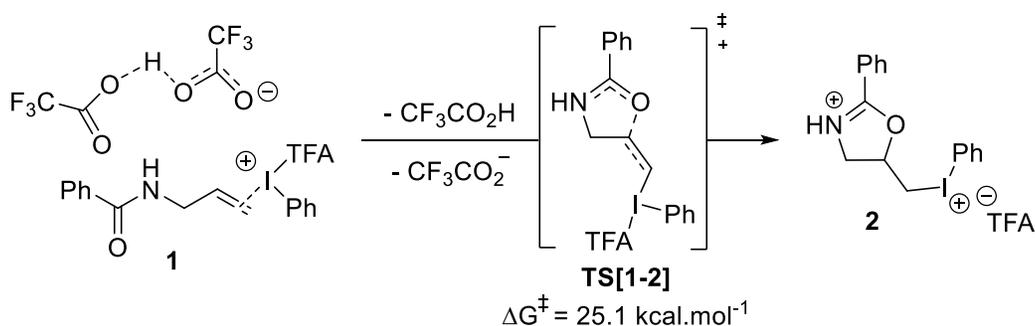
$\Delta G^{\ddagger} = 23.4$ kcal.mol^{-1} with 2-iodoanisole instead of iodobenzene

(b) This work: alkyne activation?

4, 61% yield, 14:1 d.r.
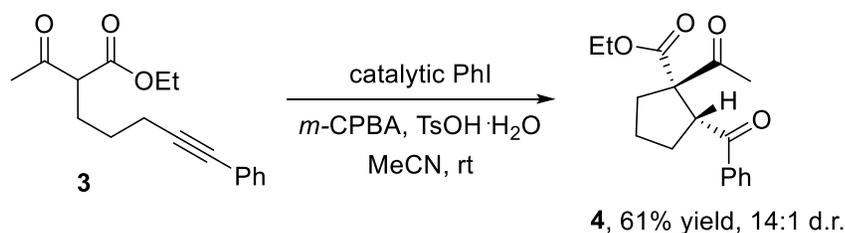
Scheme 1. (a) Our previous work demonstrating the iodoarene-catalyzed cyclization of an amide onto a pendent alkene. (b) Iodobenzene-catalyzed cyclization of a δ-alkynyl β-ketoester.

Results and Discussion

In our initial report of the cyclizations of δ-alkynyl β-ketoesters, we proposed that the alkyne activation, i.e. **5a**, was most likely, followed by cyclization by attack of the enol (Figure 1). Alternatively, formation of α-iodonium species **6a** could occur followed by *syn*-addition to the alkyne. A third possibility is the formation of iodonium bound enolate **7a** followed by nucleophilic attack of the alkyne. Functionalizations of 1,3-dicarbonyls using hypervalent iodine reagents have been proposed to proceed through formation of intermediates similar to **6**[13] and **7a**.[14] In order to determine the mode of activation of **3**, we set out to model the reaction using DFT calculations.


5a 5.4 kcal.mol^{-1}　　　　　　**6** 10.9 kcal.mol^{-1}　　　　　　**7a** 19.8 kcal.mol^{-1}
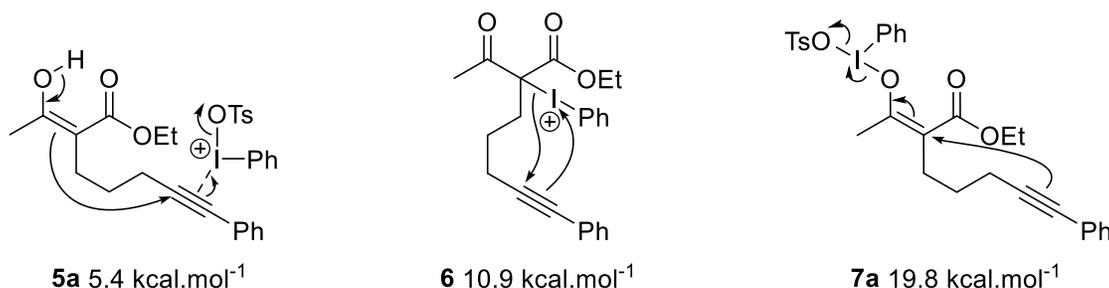
Figure 1. Three possible mechanisms of cyclization of the δ-alkynyl β-ketoester

Initial results suggested that a mechanism proceeding through intermediate **7a** was unlikely as its calculated energy was significantly higher than that for **5a** and **6**. Balanced equations for formation of **5a**, **6** and **7a** are shown in the Supplementary Material. In addition, computed values with a hydroxy ligand on the iodine rather than the tosylate were higher (details in the Supplementary Material).

Based on these initial findings, we decided to focus our efforts on cyclization occurring through intermediates **5a** and **6** (Figure 2). Starting from Koser's reagent **8**, which is formed under the reaction conditions, loss of hydroxide occurs to form cationic **9a**. This species can either coordinate to the alkyne of **3'** or bond to the carbon between the two carbonyls. In solution, the β-ketoester **3** prefers to exist in its tautomeric form **3'**.

Experiments to connect acyclic **6** to cyclic **10a** by insertion of the alkyne into the C-I bond were unsuccessful. However, the cyclization of the activated alkyne intermediate **5a** was found to be possible in both a *syn*- and an *anti*-fashion. Moreover, it was found that the *anti*-addition is far lower in energy than the *syn*-addition (12.7 versus 23.9 kcal.mol^{-1}). It is notable that this cyclization is particularly facile, especially compared to the cyclization of **1** where $\Delta G^{\ddagger}$ = 25.1 kcal.mol^{-1} (with iodobenzene derived mediator). Subsequent loss of iodobenzene generates carbocation **11** followed by addition of water and tautomerization to furnish the final product **4**. Efforts to connect **10b** to **4** without formation of the carbocation **11** were not fruitful. The major diastereomer of the final product, **4**, is 3.2 kcal.mol^{-1} more stable than the minor diastereomer **13**.
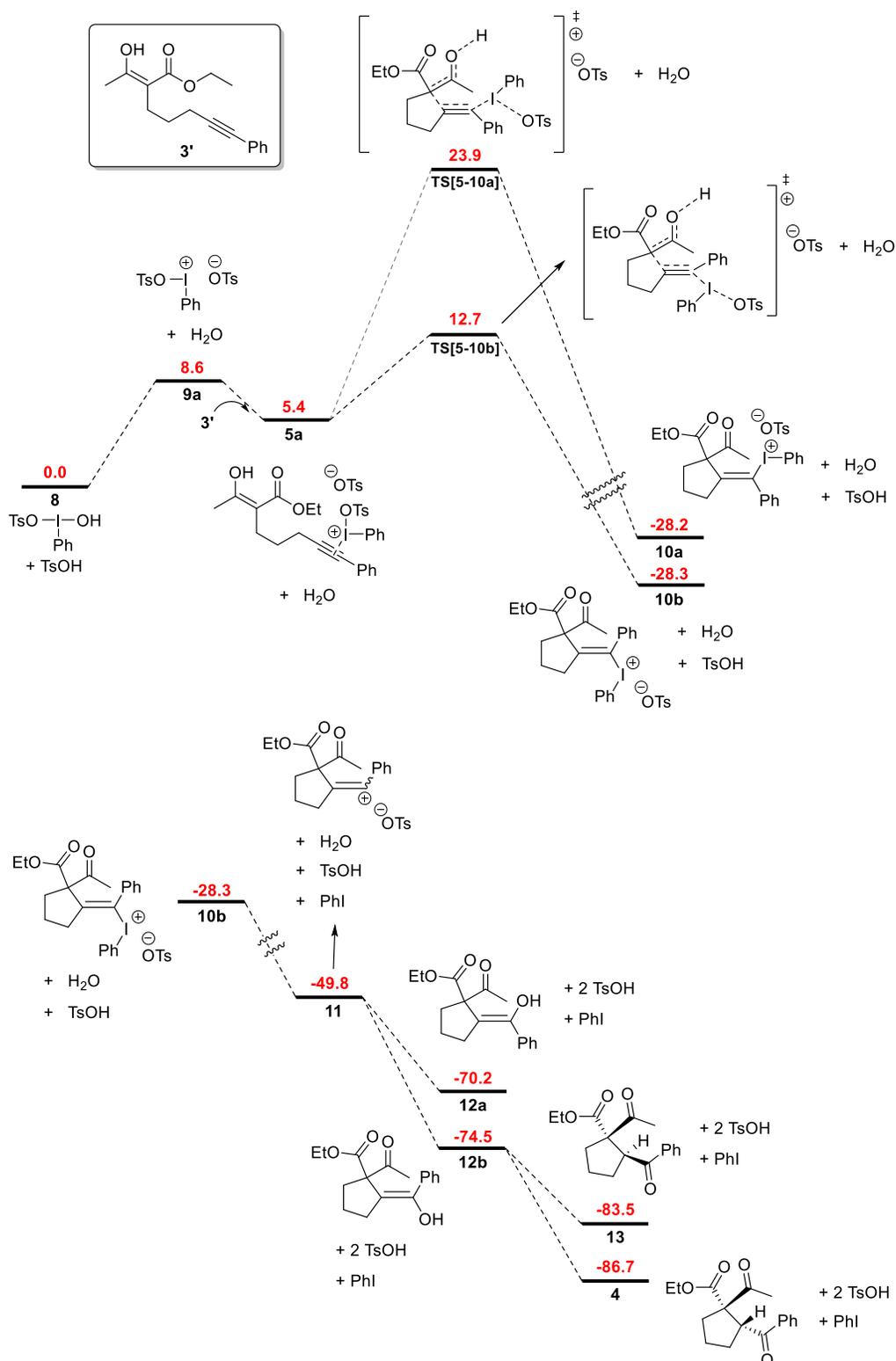
Figure 2. Calculated potential energy profile for the Koser's reagent **8** mediated cyclization of alkyne **3'**. Free energies are reported in kcal.mol^{-1}.

The structures in the mechanism have been connected through forward and reverse IRC calculations and the optimized geometries of all intermediates and transition states were as expected (Figure 3). In our 2011

report, we noted that deprotonation of **4** was not possible under a variety of conditions. We hypothesized that the α-proton to the ketone was not aligned with the carbonyl π* orbital. Our present study supports this hypothesis as the H-C-C-O angle is 173° in the optimized structure.
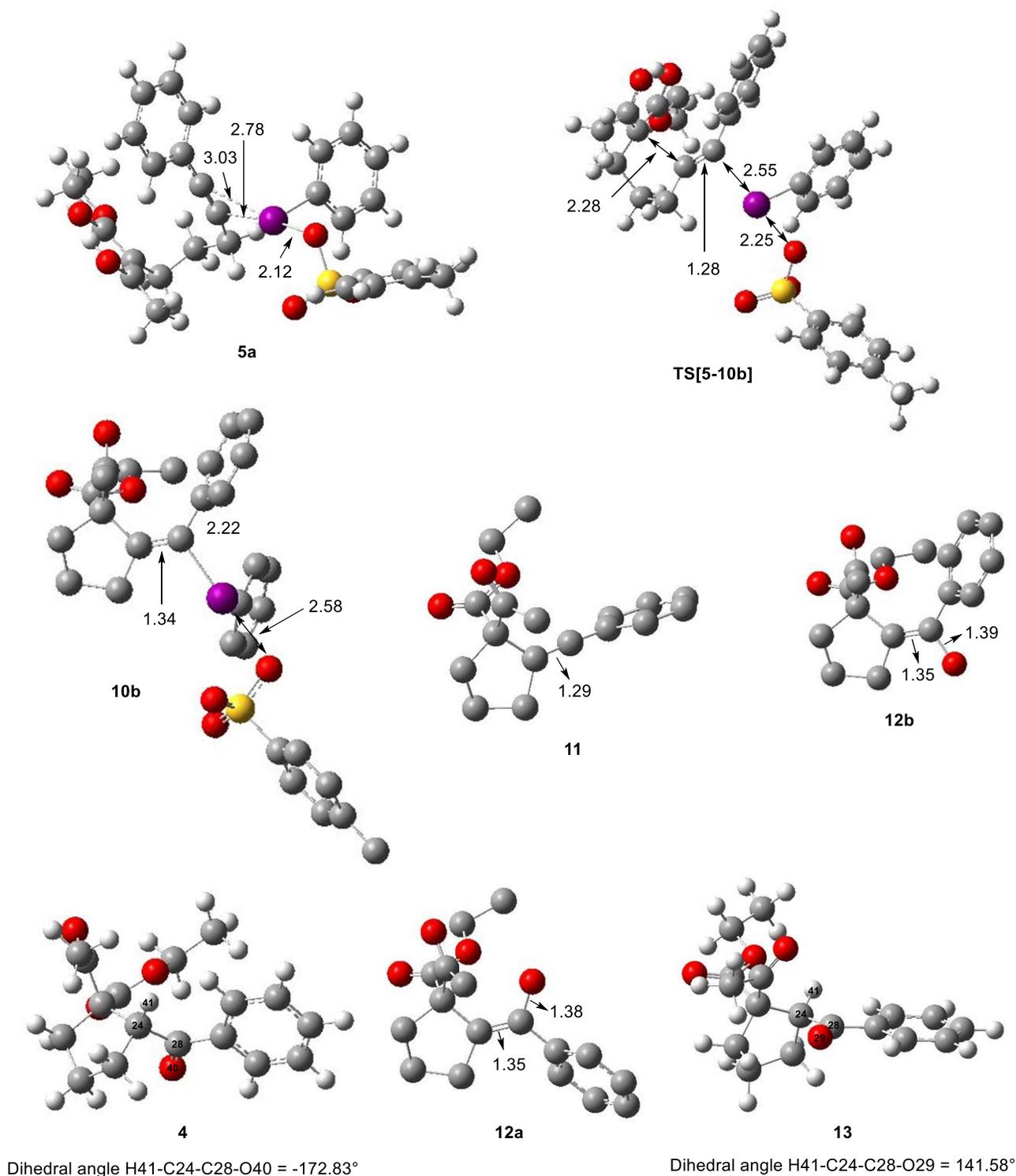
Figure 3. Optimized geometries for intermediates and transition state. All the bond lengths are given in Angstroms.

Conclusions

The mechanism of the cyclization of a δ-alkynyl β-ketoester with hypervalent iodine has been shown to proceed though activation of the alkyne by DFT modelling. Hypervalent iodine mediated formation of C-C bonds is relatively uncommon compared to the construction of C-X bonds. We hope that the mechanistic details revealed in this study help to inspire creativity in synthetic chemistry.

Experimental Section

Quantum chemical calculations were performed using Gaussian 16,[15] and GaussView was used for molecular modelling.[16] The geometry optimizations were performed in the gas phase under standard conditions using DFT[17-19] in combination with the 6-31+G(d,p)[20] basis set for all atoms except iodine, for which the SDD (Stuttgart/Dresden) effective core potential was used.[21] Exhaustive conformation search was carried out on all the species described and only the lowest energy conformation is presented in the mechanistic scheme. All the bond lengths are given in Angstroms. Vibrational frequency calculations were performed in order to determine the imaginary frequencies for the respective molecules. The imaginary frequencies verified whether the stationary points are minima, having no imaginary frequencies, or transition states, possessing one imaginary frequency. The connectivity of the transition states was confirmed by computing IRC (intrinsic reaction coordinate) from the transition-state geometry towards both the reactant and product.[22,23]

Solvent effects were taken into account using the conductor-like polarizable continuum model (CPCM).[24] Single-point calculations on the gas-phase optimized geometries were performed to estimate the change in energy in the presence of the solvent, acetonitrile. The triple-zeta quality 6-311++G(d,p) basis set along with SDD for I was used to account for the solvent effects. The Gibbs free energy values provided in the text are Gibbs energy in solution, G_{sol}, which was calculated by adding the thermochemistry corrections, G-E, to the refined single point energies, E_{sol}, i.e., $G_{sol} = E_{sol} + G - E$. The sums of the electronic and thermal free energies (G) for reactants and transition states were obtained by the standard procedure in the framework of the harmonic approximation. The $\Delta G^{\ddagger}$ of the reactions was calculated from the differences in the G values of the transition states and the reactants.

Acknowledgements

Supplementary Material

Cartesian coordinates and energies of all calculated structures.

References

1. Grelier, G.; Darses, B.; Dauban, P. *Beilstein J. Org. Chem.* **2018**, *14*, 1508–1528.
https://doi.org/10.3762/bjoc.14.128

2. Yoshimura, A.; Zhdankin, V. V. *Chem. Rev.* **2016**, *116*, 3328–3435.
https://doi.org/10.1021/acs.chemrev.5b00547

3. Zheng, Z. S.; Zhang-Negrerie, D.; Du, Y. F.; Zhao, K. *Sci. China: Chem.* **2014**, *57*, 189–214.
https://doi.org/10.1007/s11426-013-5043-1

4. Zhdankin, V. V. *Hypervalent Iodine Chemistry: Preparation, Structure, and Synthetic Applications of Polyvalent Iodine Compounds*; Wiley: New York, 2013.
https://doi.org/10.1002/9781118341155

5. Sreenithya, A.; Surya, K.; Sunoj, R. B. *WIREs Comput. Mol. Sci.* **2017**, *7*, e1299. 10.1002/wcms.1299.
https://doi.org/10.1002/wcms.1299

6. Sun, T.-Y.; Chen, K.; Lin, Q.; You, T.; Yin, P. *Phys. Chem. Chem. Phys.* **2021**, *23*, 6758-6762.
https://doi.org/10.1039/D0CP06692C

7. Robidas, R.; Huber, S. M.; Legault, C. Y. *Arkivoc* **2021**, *vii*, 128-140.
https://doi.org/10.24820/ark.5550190.p011.639

8. Ganji, B.; Ariafard, A. *Org. Biomol. Chem.* **2019**, *17*, 3521-3528.
https://doi.org/10.1039/C9OB00028C

9. Alhalib, A.; Kamouka, S.; Moran, W. J. *Org. Lett.* **2015**, *17*, 1453-1456.
https://doi.org/10.1021/acs.orglett.5b00333

10. Butt, S. E.; Das, M.; Sotiropoulos, J.-M.; Moran, W. J. *J. Org. Chem.* **2019**, *84*, 15605-15613.
https://doi.org/10.1021/acs.joc.9b02623

11. Rodríguez, A.; Moran, W. J. *Org. Lett.* **2011**, *13*, 2220-2223.
https://doi.org/10.1021/ol200471w

12. Hyatt, I. F. D.; Dave, L.; David, N.; Kaur, K.; Medard, M.; Mowdawalla, C. *Org. Biomol. Chem.* **2019**, *17*, 7822-7848.
https://doi.org/10.1039/C9OB01267B

13. Yu, J.; Tian, J.; Zhang, C. *Adv. Synth. Catal.* **2010**, *352*, 531 – 546.
https://doi.org/10.1002/adsc.200900737

14. Martins, B. S.; Kaiser, D.; Bauer, A.; Tiefenbrunner, I.; Maulide, N. *Org. Lett*. **2021**, *23*, 2094–2098.
https://doi.org/10.1021/acs.orglett.1c00251

15. Gaussian 16, Revision C.01, Frisch, M. J.; Trucks, G. W.; Schlegel, H. B.; Scuseria, G. E.; Robb, M. A.; Cheeseman, J. R.; Scalmani, G.; Barone, V.; Petersson, G. A.; Nakatsuji, H.; Li, X.; Caricato, M.; Marenich, A. V.; Bloino, J.; Janesko, B. G.; Gomperts, R.; Mennucci, B.; Hratchian, H. P.; Ortiz, J. V.; Izmaylov, A. F.; Sonnenberg, J. L.; Williams-Young, D.; Ding, F.; Lipparini, F.; Egidi, F.; Goings, J.; Peng, B.; Petrone, A.; Henderson, T.; Ranasinghe, D.; Zakrzewski, V. G.; Gao, J.; Rega, N.; Zheng, G.; Liang, W.; Hada, M.; Ehara, M.; Toyota, K.; Fukuda, R.; Hasegawa, J.; Ishida, M.; Nakajima, T.; Honda, Y.; Kitao, O.; Nakai, H.; Vreven, T.; Throssell, K.; Montgomery, J. A., Jr.; Peralta, J. E.; Ogliaro, F.; Bearpark, M. J.; Heyd, J. J.; Brothers, E. N.; Kudin, K. N.; Staroverov, V. N.; Keith, T. A.; Kobayashi, R.; Normand, J.; Raghavachari, K.; Rendell, A. P.; Burant, J. C.; Iyengar, S. S.; Tomasi, J.; Cossi, M.; Millam, J. M.; Klene, M.; Adamo, C.; Cammi, R.; Ochterski, J. W.; Martin, R. L.; Morokuma, K.; Farkas, O.; Foresman, J. B.; Fox, D. J. 2016

16. GaussView, Version 5, Dennington, Roy; Keith, Todd A.; Millam, John M. Semichem Inc., Shawnee Mission, KS, 2016.

17. Becke, A. D. *J. Chem. Phys.* **1993**, *98*, 1372-1377.

https://doi.org/10.1063/1.464304

18. Becke, A. D. *Phys. Rev. A.* **1988**, *38*, 3098.

https://doi.org/10.1103/PhysRevA.38.3098

19. Lee, C.; Yang, W.; Parr, R. G. *Phys. Rev. B: Condens. Matter,* **1988**, *37*, 785.

https://doi.org/10.1103/PhysRevB.37.785

20. Hariharan, P. C.; Pople, J.A. *Theoret. Chim. Acta.* **1973**, *28*, 213-222.

https://doi.org/10.1007/BF00533485

21. Igel-Mann, G.; Stoll, H., Preuss, H. *Mol. Phys.* **1988**, *65,* 1321-1328.

https://doi.org/10.1080/00268978800101811

22. Gonzalez, C.; Schlegel, H. B. *J. Chem. Phys.* **1989**, *90*, 2154-2161.

https://doi.org/10.1063/1.456010

23. Gonzalez, C.; Schlegel, H. B. *J. Phys. Chem.* **1990**, *94, 5523-5527.*

https://doi.org/10.1021/j100377a021

24. Cossi, M.; Rega, N.; Scalmani, G.; Barone, V. *J. Comput. Chem.* **2003**, *24,* 669-681.

https://doi.org/10.1002/jcc.10189